

## Similarity and dissimilarity in correlations of genomic DNA

Boris Podobnik<sup>a,b</sup>, Jia Shao<sup>c</sup>, Nikolay V. Dokholyan<sup>d</sup>, Vinko Zlatic<sup>e,\*</sup>,  
H. Eugene Stanley<sup>c</sup>, Ivo Grosse<sup>f</sup>

<sup>a</sup>Faculty of Civil Engineering, University of Rijeka, Rijeka, Croatia

<sup>b</sup>Zagreb School of Economics and Management, Zagreb, Croatia

<sup>c</sup>Center for Polymer Studies and Department of Physics, Boston University, Boston, USA

<sup>d</sup>School of Medicine, University of North Carolina, Chapel Hill, USA

<sup>e</sup>Rudjer Boskovic Institute, Zagreb, Croatia

<sup>f</sup>Leibniz Institute of Plant Genetics and Crop Plant Research (IPK), Gatersleben, Germany

Available online 21 June 2006

### Abstract

We analyze auto-correlations of human chromosomes 1–22 and rice chromosomes 1–12 for seven binary mapping rules and find that the correlation patterns are different for different rules but almost identical for all of the chromosomes, despite their varying lengths and GC contents. We propose a simple stochastic process for modeling these correlations, and we find that the proposed process can reproduce, quantitatively and qualitatively, the correlation patterns found in the genomes of human and rice.

© 2006 Elsevier B.V. All rights reserved.

PACS: 87.10; 05.40.+j

DNA is the carrier of genetic information of many living organisms. It is comprised of the four nucleotides A, T, C, and G. In order to study correlations in DNA sequences one commonly maps each nucleotide to a binary number and then studies correlations in the resulting numerical sequence. There are three different partitions of four nucleotides into two subsets of two nucleotides each, and so there are three different binary mapping rules that map a nucleotide  $s$  onto a binary number  $x \in \{-1, +1\}$ :

- SW rule:  $x = 1$  for C or G, and  $x = -1$  otherwise.
- KM rule:  $x = 1$  for A or C, and  $x = -1$  otherwise.
- RY rule:  $x = 1$  for A or G, and  $x = -1$  otherwise.

There are many studies on long-range correlations in various DNA sequences using different binary representations of the four nucleotides [1–12] with partially contradicting results. As it is possible that a symbolic sequence shows long-range correlations for one rule and no correlations for another rule, we conjecture that some of these apparent contradictions might be due to the fact that different research groups

\*Corresponding author.

E-mail addresses: [jiashao@buphy.bu.edu](mailto:jiashao@buphy.bu.edu) (J. Shao), [vzlatic@irb.hr](mailto:vzlatic@irb.hr) (V. Zlatic).

have chosen different binary mapping rules. In the following, we analyze long-range correlations in DNA sequences using each of the three binary mapping rules.

First, we map a DNA sequence  $(s_0, s_1, \dots, s_{N-1})$  of length  $N$  to a binary sequence  $(x_0, x_1, \dots, x_{N-1})$  by one of the three binary mapping rules. Then, we compute correlations by employing the *detrended fluctuation analysis* (DFA) [13], a variant of the root-mean-square analysis of a random walk. In the DFA method, one measures the standard deviation  $F(\ell)$  of the detrended fluctuations within a window of length  $\ell$  as a function of  $\ell$  [14]. If the auto-correlation function  $C(\ell) \equiv \langle x_n x_{n+\ell} \rangle - \langle x_n \rangle \langle x_{n+\ell} \rangle$  can be approximated by a power-law with exponent  $\gamma$ , i.e., if  $C(\ell) \propto \ell^{-\gamma}$ , then  $F(\ell)$  can be approximated by a power-law with exponent  $\alpha$ , i.e.,  $F(\ell) \propto \ell^\alpha$ , with  $\alpha \approx 1 - \gamma/2$  [15]. If  $\alpha > 0.5$ , the time series is power-law correlated; if  $\alpha = 0.5$ , the time series is uncorrelated or short-range correlated; and if  $\alpha < 0.5$ , the time series is power-law anti-correlated.

By using the DFA method, we analyze auto-correlations in two completely sequenced genomes, one from the animal kingdom and one from the plant kingdom. Fig. 1(a) shows  $F(\ell)$  versus  $\ell$  for all 22 autosomes of *Homo sapiens* using the SW rule, the KM rule, and the RY rule [16]. First, we find that for each binary mapping rule the  $F(\ell)$  curves corresponding to different chromosomes are almost identical. Second, we find in agreement with Ref. [17,18] that for the SW rule the  $F(\ell)$  curves can be approximated by a power-law with scaling exponent  $\alpha \rightarrow 1$  for scales  $\ell$  exceeding  $10^6$  bp, corresponding to  $1/f$  noise. Third, we find that for the KM rule and the RY rule the  $F(\ell)$  curves can also be approximated by power-laws, but with scaling exponents  $\alpha_{KM}$  and  $\alpha_{RY}$  that are substantially smaller than  $\alpha_{SW}$ , i.e.,  $\alpha_{SW} > \alpha_{KM} \approx \alpha_{RY}$ .

In view of the many known differences among the 22 autosomes of *Homo sapiens* it is surprising that their auto-correlations are almost indistinguishable. In order to study if the phenomenon that auto-correlations of different chromosomes are almost indistinguishable whereas auto-correlations of different binary mapping rules are different from each other is ubiquitous, we analyze all 12 autosomes of *Oryza sativa* using the SW rule, the KM rule, and the RY rule. From Fig. 1(b) we find that for each binary mapping rule the  $F(\ell)$  curves corresponding to different chromosomes are almost indistinguishable. We find that the  $F(\ell)$  curves for the KM rule and the RY rule can be approximated by a power-law with almost the same scaling exponent, i.e.,  $\alpha_{KM} \approx \alpha_{RY}$ , and that for the SW rule there is a significant crossover in the  $F(\ell)$  curves at approximately  $\ell \approx 10^4$  bp. In agreement to Fig. 1(a) we find that also for rice the scaling exponent  $\alpha_{SW}$  is greater than  $\alpha_{KM} \approx \alpha_{RY}$  in the asymptotic regime.

In summary, we find that the  $F(\ell)$  curves for all chromosomes are (i) identical and (ii) can be approximated by power-laws for each rule, (iii) the power-law for the SW rule is different from the power-laws for the KM rule and the RY rule, and (iv) the power-laws for the KM rule and the RY rule are almost identical.

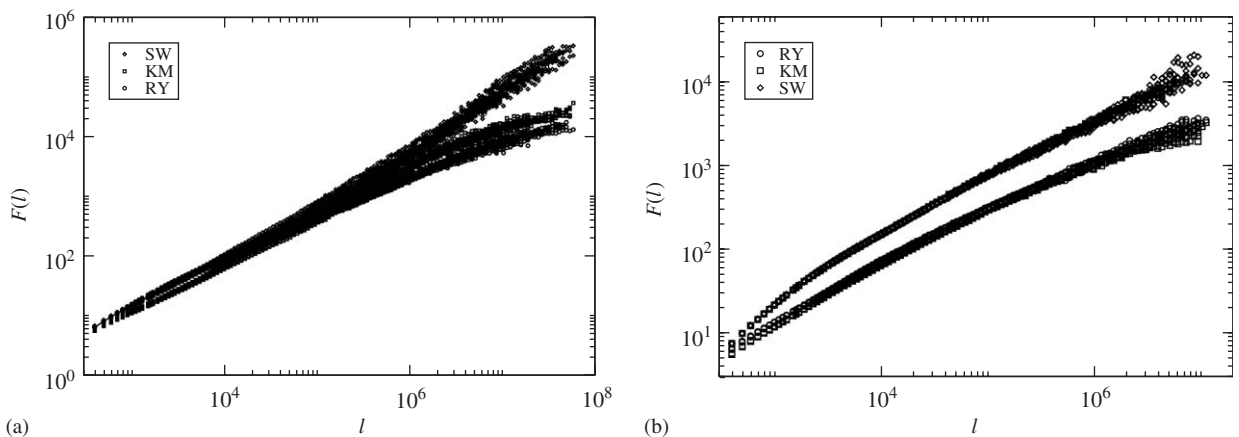


Fig. 1. Detrended fluctuation functions  $F(\ell)$  versus  $\ell$ . For the SW rule, the KM rule, and the RY rule we show the  $F(\ell)$  curves (a) for all 22 human chromosomes (autosomes) and (b) for rice. For both human and rice, the  $F(\ell)$  curves for each rule practically overlap. (a) For human, we find for the SW rule that the  $F(\ell)$  curves tend to  $1/f$  noise for very large scales. For very large scales we find  $\alpha_{KM} \approx \alpha_{RY} < \alpha_{SW}$ . (b) For rice, we find that the  $F(\ell)$  curves for the KM rule and the RY rule collapse onto each other, and for large scales we find  $\alpha_{KM} \approx \alpha_{RY} < \alpha_{SW}$ .

Several stochastic models have been proposed to generate long-range correlations, but most of them are focused on reproducing correlations for only one binary mapping rule [6,19]. In order to model the scaling properties observed in the genomes of human and rice, we proceed in two steps. First, we introduce two mutually independent ARFIMA processes [20,21]  $z_n^{(\text{SW})}$  and  $z_n^{(\text{KM})}$  defined by [22]

$$z_n^{(j)} = \sum_{\ell=1}^{\infty} a_{\ell}(\rho_j) z_{n-\ell}^{(j)} + e_n^{(j)}, \tag{1a}$$

$$a_{\ell}(\rho_j) = \frac{\Gamma(\ell - \rho_j)}{\Gamma(-\rho_j)\Gamma(1 + \rho_j)}, \tag{1b}$$

where  $j \in \{\text{sw}, \text{km}\}$ ,  $e_n^{(j)}$  are independent and identically distributed Gaussian variables,  $\Gamma$  denotes the Gamma function, and each stochastic process  $z_n^{(j)}$  is parameterized by one parameter  $\rho_j \in (-0.5, 0.5)$ . Second, we define the nucleotide

$$s_n = \begin{cases} \text{A} & \text{if } z_n^{(\text{SW})} < \delta \wedge z_n^{(\text{KM})} < 0, \\ \text{T} & \text{if } z_n^{(\text{SW})} < \delta \wedge z_n^{(\text{KM})} > 0, \\ \text{G} & \text{if } z_n^{(\text{SW})} > \delta \wedge z_n^{(\text{KM})} < 0, \\ \text{C} & \text{if } z_n^{(\text{SW})} > \delta \wedge z_n^{(\text{KM})} > 0, \end{cases} \tag{2}$$

where  $\delta$  is a cutoff value controlling the excess of GC over AT nucleotides. This assignment can be interpreted in terms of two spin models, where each nucleotide is represented by two spins, one spin corresponding to the sw state of the nucleotide, and the other spin corresponding to the km state of the nucleotide.

To simulate DNA sequences we choose two ARFIMA processes due to the fact that the ARFIMA process generates power-law correlated time series  $z_n^{(j)}$  with scaling exponent  $\alpha_j \approx 1 + \rho_j$  [20,21,23,24]. We find by numerical simulations that the scaling relation  $\alpha_j \approx 1 + \rho_j$  also holds for the time series  $\text{sgn}(z_n^{(j)})$ . Hence, two ARFIMA processes running simultaneously generate sequences with  $\alpha_{\text{SW}} \approx 1 + \rho_{\text{SW}}$  and  $\alpha_{\text{KM}} \approx 1 + \rho_{\text{KM}}$ .

If  $\delta$  in the above equation is chosen to be zero, the probability of occurrence of each nucleotide is identical to 0.25, due to the choice of mutually independent variables  $e_{n^{(j)}}$  in Eq. (1) drawn from a symmetrical Gaussian distribution.

The relative frequency of nucleotides c and G is equal ( $\approx 0.21$  for chromosome 1), and the same holds for A and T ( $\approx 0.28$  for chromosome 1). To obtain the two model parameters,  $p_S \equiv P(z_n^{(\text{SW})} > \delta)$  and  $p_K \equiv P(z_n^{(\text{KM})} > 0)$ , we equate the relative frequency of nucleotide A  $\equiv (-1, +1)$  with  $p_W \cdot p_K$ , T  $\equiv (-1, -1)$  with  $p_W \cdot p_M$ , C  $\equiv (+1, +1)$  with  $p_S \cdot p_K$ , and G  $\equiv (+1, -1)$  with  $p_S \cdot p_M$ . From these equations and by using the obvious relations,  $p_W = 1 - p_S$  and  $p_M = 1 - p_K$ , we easily obtain  $p_A = 0.5$  and  $p_W = 0.582$  for chromosome 1. Thus, asymmetry is needed only for the sw rule, in accordance to the Chargaff rule.

For this simple model, one can easily derive the auto-correlation function for the RY rule

$$C_{\text{RY}}(\ell) = 4C_{\text{SW}}(\ell)C_{\text{KM}}(\ell) + C_{\text{SW}}(\ell)(p_K - p_M)^2 + C_{\text{KM}}(\ell)(p_W - p_S)^2, \tag{3}$$

where for  $p_K \approx p_M$  and  $p_W \neq p_S$ , which is the case for DNA sequences,  $C_{\text{RY}}(\ell)$  reduces to  $C_{\text{KM}}(\ell)(p_W - p_S)^2$ , implying

$$\alpha_{\text{RY}} \approx \alpha_{\text{KM}}. \tag{4}$$

Hence, the model predicts that  $C_{\text{RY}}(\ell)$  shows the same scaling behavior as  $C_{\text{KM}}(\ell)$ . Interestingly, this behavior predicted for the model for asymptotically large  $\ell$  is observed in real DNA (Fig. 1).

We perform numerical simulations with  $\rho_{\text{SW}} = 0.41$  and  $\rho_{\text{KM}} = 0.25$  in order to reproduce the observed power-law correlations of the human sw and km rule, respectively, shown in Fig. 2(a). We generate a sequence of length  $N = 2 \times 10^7$  bp and compute  $F(\ell)$ , for  $\ell$  ranging from  $\ell = 10^3$  to  $10^7$  bp (asymptotic regime). In Fig. 2(b) we show  $F(\ell)$  for the sw, the km, and the RY binary mapping rules. The model gives that  $F(\ell)$  calculated for the sw rule and the km rule are power-laws as expected, and it predicts that also RY correlations can be approximated by a power-law with an exponent given by Eq. (4). Next we perform numerical simulations with  $\rho_{\text{SW}} = 0.1$  and  $\rho_{\text{KM}} = 0.0$  in order to reproduce power-law correlations of the rice sw and km

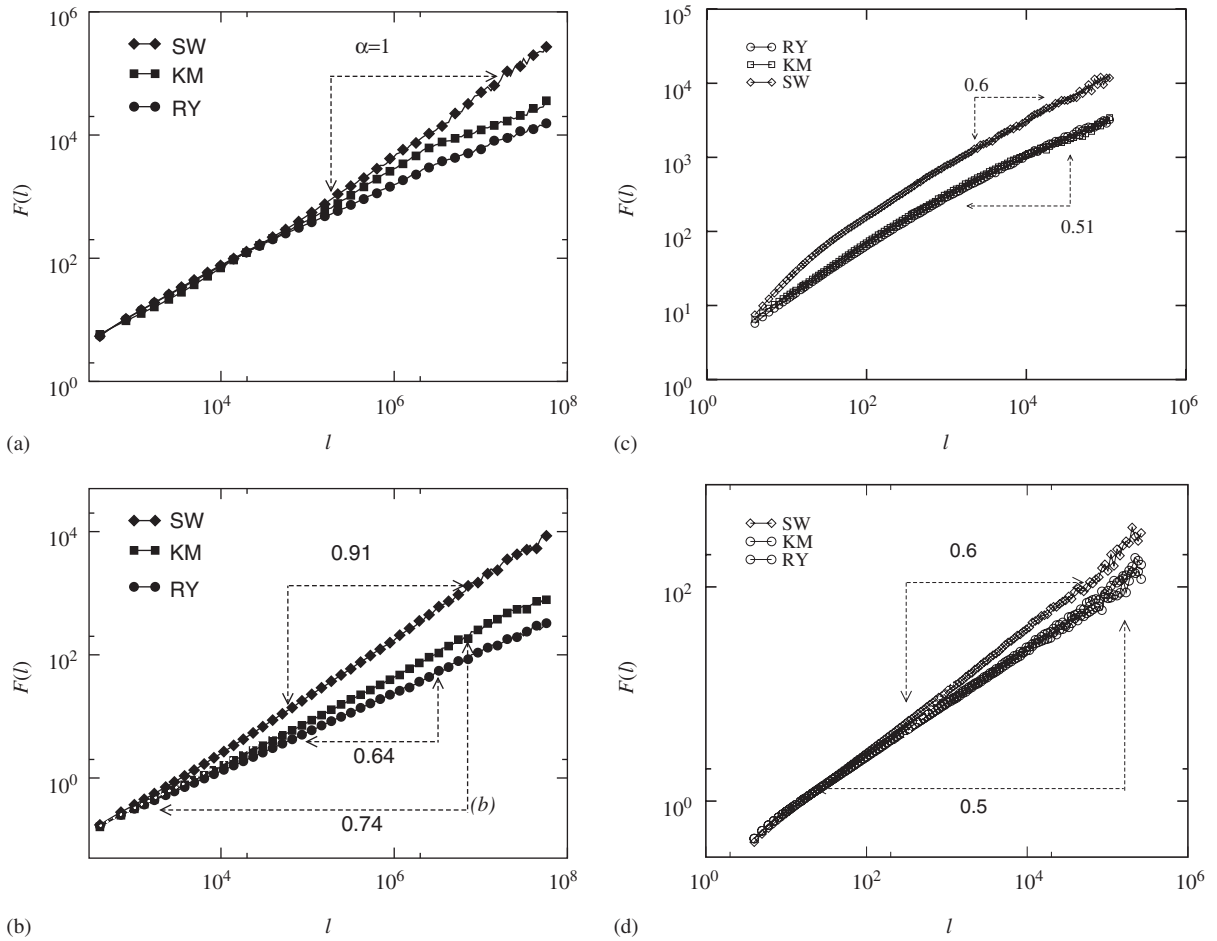


Fig. 2.  $F(\ell)$  versus  $\ell$ . (a) For human chromosome 1, we find that the  $F(\ell)$  functions for the KM rule and the RY rule are approximately the same for very large scales, whereas for the SW rule the scaling of  $F(\ell)$  corresponds to  $1/f$  noise [17]. (b) Model simulations. For parameters  $\alpha_{\text{SW}} = 0.41$  and  $\alpha_{\text{KM}} = 0.25$  set to fit the scaling for the whole range for the SW rule and the KM rule, and the cutoff value  $\delta = 0.2$  set to model “AT rich” DNA, we perform numerical simulations and generate the sequences for different rules. We find the model reproduces the correlations found in the empirical data. (c–d) For rice, we find again that the  $F(\ell)$  curves for the KM rule and the RY rule are practically identical, that  $\alpha_{\text{SW}} > \alpha_{\text{KM}} \approx \alpha_{\text{RY}}$ , and that the model can reproduce the correlations found in the empirical data.

rule, shown in Fig. 2(c). Fig. 2(d) shows that  $F(\ell)$  for the SW rule can be approximated by a power-law, while for the KM rule and the RY rule there are almost no correlations, consistent with the findings of Fig. 2(c).

In order to test the validity of the model, we compute the auto-correlation functions for the following four binary mapping rules:

- $A\bar{A}$  rule:  $x = 1$  for A, and  $x = -1$  otherwise.
- $G\bar{G}$  rule:  $x = 1$  for G, and  $x = -1$  otherwise.
- $C\bar{C}$  rule:  $x = 1$  for C, and  $x = -1$  otherwise.
- $T\bar{T}$  rule:  $x = 1$  for T, and  $x = -1$  otherwise.

For the model one can easily compute

$$C_{A\bar{A}}(\ell) = C_{\text{SW}}(\ell)C_{\text{KM}}(\ell) + C_{\text{SW}}(\ell)p_M^2 + C_{\text{KM}}(\ell)p_W^2, \tag{5a}$$

$$C_{T\bar{T}}(\ell) = C_{SW}(\ell)C_{KM}(\ell) + C_{SW}(\ell)p_K^2 + C_{KM}(\ell)p_W^2, \tag{5b}$$

$$C_{C\bar{C}}(\ell) = C_{SW}(\ell)C_{KM}(\ell) + C_{SW}(\ell)p_M^2 + C_{KM}(\ell)p_S^2, \tag{5c}$$

$$C_{G\bar{G}}(\ell) = C_{SW}(\ell)C_{KM}(\ell) + C_{SW}(\ell)p_K^2 + C_{KM}(\ell)p_S^2. \tag{5d}$$

One can also derive that the following relations among the scaling exponents hold for all  $N \in \{A, T, C, G\}$ :

$$\alpha_{N\bar{N}} = \max(\alpha_{SW}, \alpha_{KM}). \tag{6}$$

If  $\alpha_{SW} > \alpha_{KM}$ , one can easily show that  $C_{N\bar{N}}(\ell)$  scales as  $C_{SW}(\ell)$ , i.e.,  $\alpha_{N\bar{N}} \approx \alpha_{SW}$ . This implies that for asymptotically large  $\ell$ ,  $C_{N\bar{N}}(\ell)$  has the same scaling behavior as  $C_{SW}(\ell)$ . All of the analytical derivations only assume that there are two binary mapping rules characterized by power-law correlations.

In order to test if these predictions can possibly be observed in real DNA, we show in Fig. 3(a)  $F(\ell)$  for all four  $N\bar{N}$  rules for all human autosomes. Interestingly, the  $F(\ell)$  curves are identical for all autosomes and for all rules and can be approximated by a single power-law with exponent  $\alpha_{SW}$ . Fig. 3(c) shows that the same scaling behavior holds for the rice chromosomes, i.e., the  $F(\ell)$  curves for all chromosomes and for all four  $N\bar{N}$  rules are almost identical and can be approximated by a single power-law. Next we perform numerical simulations and generate sequences for all four  $N\bar{N}$  rules based on the parameters in Fig. 2. For the human autosomes in Fig. 3(c) and for the rice chromosomes in Fig. 3(d), we find that the  $F(\ell)$  curves for the  $N\bar{N}$  rules are the same and similar to the real data. Thus, the model based on two ARFIMA processes is capable of reproducing, qualitatively and to a large extent also quantitatively, the power-law correlations in human and rice DNA.

In future work, it would be worthwhile to put some effort into combining the proposed model with Markov models [25–29] with the goal of increasing their predictive power in a variety of bioinformatics applications.

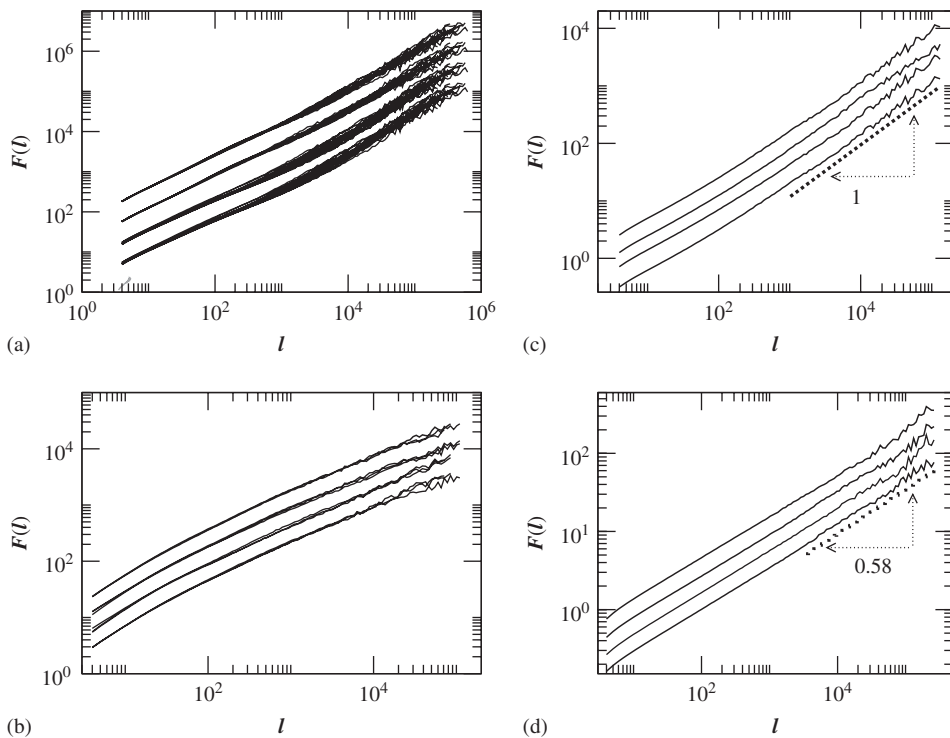


Fig. 3.  $F(\ell)$  versus  $\ell$ . For both (a) human and (b) rice chromosomes we find that the  $F(\ell)$  curves for the  $A\bar{A}$ , the  $C\bar{C}$ , the  $G\bar{G}$ , and the  $T\bar{T}$  rule practically overlap. Curves for different rules are shifted. (c–d) Model simulations. For parameter values set in Fig. 2, we find that the  $F(\ell)$  curves for the  $A\bar{A}$ , the  $C\bar{C}$ , the  $G\bar{G}$ , and the  $T\bar{T}$  rule are identical and similar to the  $F(\ell)$  curves observed in the empirical data.

## Acknowledgments

We thank S.V. Buldyrev for valuable discussions, M. Mohr for her assistance in retrieving and processing the data, and the Ministry of Science of Croatia (Grant 0119623) and the German Federal Ministry of Education and Research (BMBF Grant 0312706A) for financial support.

## References

- [1] M. Ya Azbel, Phys. Rev. Lett. 31 (1973) 589.
- [2] E.N. Trifonov, Bull. Math. Biol. 51 (1989) 417.
- [3] C.-K. Peng, et al., Nature 356 (1992) 168.
- [4] W. Li, K. Kaneko, Europhys. Lett. 17 (1992) 655.
- [5] R. Voss, Phys. Rev. Lett. 68 (1992) 3805.
- [6] S.V. Buldyrev, et al., Phys. Rev. 47 (1993) 4514.
- [7] S.M. Osadnik, et al., Biophys. J. 67 (1994) 64.
- [8] S.V. Buldyrev, et al., Phys. Rev. 51 (1995) 5084.
- [9] H. Herzel, I. Grosse, Physica A 216 (1995) 518.
- [10] P. Bernaola-Galvan, R. Roman-Roldan, J.L. Oliver, Phys. Rev. E 53 (1996) 5181.
- [11] D. Holste, I. Grosse, H. Herzel, Phys. Rev. E 64 (2001) 041917.
- [12] D. Holste, et al., Phys. Rev. E 67 (2003) 061913.
- [13] C.-K. Peng, et al., Phys. Rev. E 49 (1994) 1685.
- [14] The auto-correlation function  $C(\ell) \equiv \langle x_n x_{n+\ell} \rangle - \langle x_n \rangle \langle x_{n+\ell} \rangle$  and the variance function  $F^2(\ell) \equiv (y_\ell - \langle y_\ell \rangle)^2$ , with  $y_\ell \equiv \sum_{n=1}^{\ell} x_n$ , are related by the Kubo formula  $F^2(\ell) = \ell C(0) + 2 \sum_{k=1}^{\ell-1} (\ell - k) C(k)$ .
- [15] Based on Ref. [14] one easily shows that, for asymptotically large sequence lengths  $N$ , if one of the functions  $F(\ell)$  or  $C(\ell)$  is of power-law form, then the other one is also of power-law form where the exponents  $\alpha$  and  $\gamma$  of the scaling relations  $F(\ell) \propto \ell^\alpha$  and  $C(\ell) \propto \ell^{-\gamma}$  are related by  $\alpha \approx 1 - \gamma/2$ .
- [16] The scaling exponents  $\alpha$  are obtained by a least-square linear regression of  $\ln F(\ell)$  versus  $\ln \ell$ . In order to make the fits  $F(\ell) \propto \ell^\alpha$  comparable for all chromosomes, we always use the same fitting region ranging from  $\ell = 10^3$  to  $10^7$  bp.
- [17] W. Li, D. Holste, Phys. Rev. E 71 (2005) 041910.
- [18] S.V. Buldyrev, Power Laws, Scale-Free Networks and Genome Biology, in: E.V. Koonin, Y.I. Wolf, G.P. Karev (Eds.), Springer Science + Business Media.
- [19] P. Allegrini, et al., Phys. Rev. 57 (1998) 4558.
- [20] C.W.J. Granger, R. Joyeux, J. Time Series Anal. 1 (1980) 15.
- [21] J. Hosking, Biometrika 68 (1981) 165.
- [22] For large values of  $\ell$ , the weights  $a_\ell(\rho_j)$  scale as  $\ell^{-1-\rho_j}$ .
- [23] B. Podobnik, et al., Phys. Rev. E 71 (2) (2005) 025104 (R).
- [24] B. Podobnik, et al., Phys. Rev. E 72 (2) (2005) 026121.
- [25] C.E. Lawrence, et al., Science 262 (1993) 208.
- [26] M. Borodovsky, D. Mcininch, Comput. Chem. 17 (1993) 123.
- [27] M. Borodovsky, et al., Nucleic Acids Res. 23 (1995) 2554.
- [28] S. Salzberg, et al., Nucleic Acids Res. 26 (1998) 544.
- [29] B. Lenhard, W.W. Wasserman, Bioinformatics 18 (2002) 1135.